Plasma Medicine 3(4): 315-332 (2013)

Nonequilibrium Atmospheric Pressure Forward-Vortex Plasma System for Generation of Reactive Species in Flowing Water for Medical Applications

Tony Liang,[a] Justine Han,[b] Selli Abdali,[c] Justin Ruegg,[b,d] & Alexander Rabinovich[e,*]

[a]Mechanical Engineering and Mechanics, Drexel University, Philadelphia, Pennsylvania, USA; [b]Advanced Plasma Solutions, Malvern, Pennsylvania, USA; [c]Biological Sciences, College of Arts and Sciences, Drexel University, Philadelphia, Pennsylvania, USA; [d]Mechanical Engineering, Rowan University, Glassboro, New Jersey, USA; [e]AJ Drexel Plasma Institute, Drexel University, Philadelphia, Pennsylvania, USA

*** Address all correspondence to:** Dr. Alexander Rabinovich, 200 Federal Street, Suite 500, Camden, NJ 08103, USA; E-mail: ar483@drexel.edu

ABSTRACT: Recent research in plasma applications in bioengineering and plasma medicine gives attention to plasma treatment of various liquids, especially water, for the growing number of medical and biological applications. In this paper we present a forward-vortex nonequilibrium atmospheric pressure plasma system for generation of nitrogen and oxygen reactive species as well as reduced pH in flowing water. We discuss the dependence of pH and nitrate produced in water on both the carrier gas and the gas feed rate.

KEY WORDS: plasmatron; gliding arc; forward-vortex; water sterilization; water cleaning

I. INTRODUCTION

There is a recent significant increase of interest in plasma treatment of various liquids, primarily water.[1–8] Dielectric barrier discharges,[3] corona discharges,[9,10] plasma jets,[8,11] thermal plasmas,[12] and other discharges[13] are being widely used for various medical, biological, chemical, and environmental applications of plasmas. Moisan et al. showed that the major contribution to effective plasma sterilization, at least in the system he describes, is by ultraviolet (UV) photons and reactive species such as atomic and molecular radicals.[14] Locke et al. discuss various discharges in liquids including electrohydraulic discharges and nonthermal plasmas for water treatment and, in particular, for applications in water cleaning.[15] Hayashi and coauthors show sterilization, especially of medical equipment, using radicals produced in the water vapor RF plasma in oxygen.[16] Kelly-Wintenberg et al. demonstrated that one atmosphere uniform glow discharge plasma (OAUGDP) exposures on a variety of surfaces have yielded reduced log numbers of bacteria, bacterial endospores, and various yeast and bacterial viruses.[17] Laroussi has found that exposure from the generation and use of a glow discharge plasma at atmospheric pressure is sufficient to destroy

the microorganisms living in an exposed medium, without damaging the medium itself.[18] Yong et al. have shown that an underwater electrical discharge in a narrow dielectric capillary produces atomic oxygen, atomic hydrogen, and hydroxyl radicals from dissociation of water vapor which also, in a bactericidal test in normal saline solution, showed that more than 99.6% of the bacterial cells were killed within 8 s, resulting from chlorine-containing species.[19] Han et al. analyzed that argon plasma jets can penetrate deep into ambient air and create a path for oxygen radicals to sterilize microbes, thereby noting its capability to clean surfaces.[20] Lee et al. have demonstrated that the sterilizing effect of atmospheric-pressure cold plasma (APCP) utilizing helium/oxygen was not due to UV light, which is known to be the major sterilization factor of APCP, but instead results from the action of reactive oxygen radicals.[21] Cvelbar et al. have determined that the results from oxygen plasma glow discharge showed that the sterilization efficiency is not necessarily just the effect of oxygen plasma radical interactions, but also of the sample heating due to radical interaction with the substrate.[22] The key question raised in most of the treatments is the scalability of the proposed technology to the industrially viable volumes of water. In this paper we present a nonequilibrium atmospheric pressure forward-vortex plasma system that we use for treatment of flowing water. This water can then be used for the ever-expanding list of medical and biological applications and can be tuned for the specific desired effect.

II. MATERIALS AND METHODS

A. Plasmatron System Design

A three-dimensional drawing of the forward-vortex gliding arc discharge system is shown in Figs. 1 and 2. The system is comprised of the two stainless steel pipes, of 1-inch outside diameter, separated by a few millimeters (can be adjusted). Air or other carrier gases are injected tangentially between the high voltage (top) and ground (bottom) electrodes. The water is injected through a pipe placed in the center of the high voltage electrode. Applied voltage and current, length of the high voltage and grounded pipes, and the liquid flow rate can all be adjusted to satisfy the specific experimental design. Note that the high voltage pipe is closed on top, creating a forward-vortex geometry.

B. Electrical Characterization

To perform an electrical analysis of the system, a Tektronix P6015a High Voltage Probe 1000X was utilized to measure voltage delivered to the plasmatron from the power supply and a Rogowski coil, 1 V, 1 A, was used to measure current output. Both the voltage probe and the Rogowski coil were connected to a Tektronix TDS

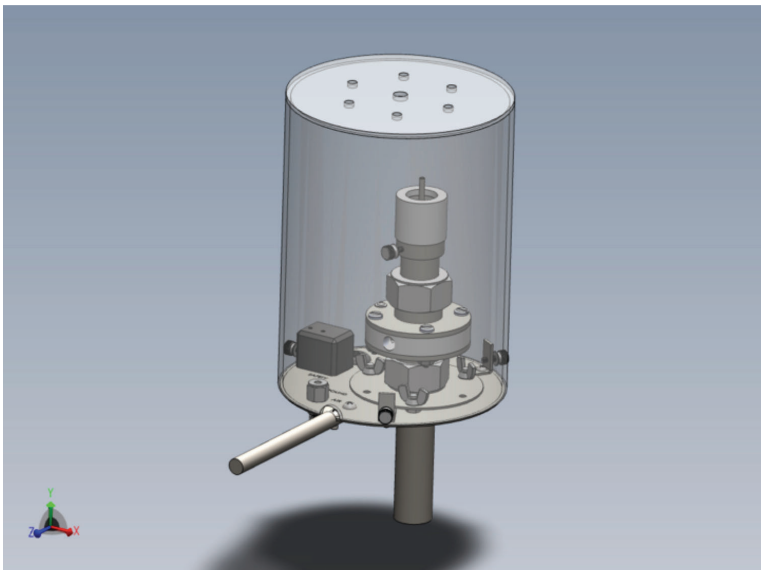

FIG. 1: Three-dimensional drawing of the forward-vortex plasmatron system

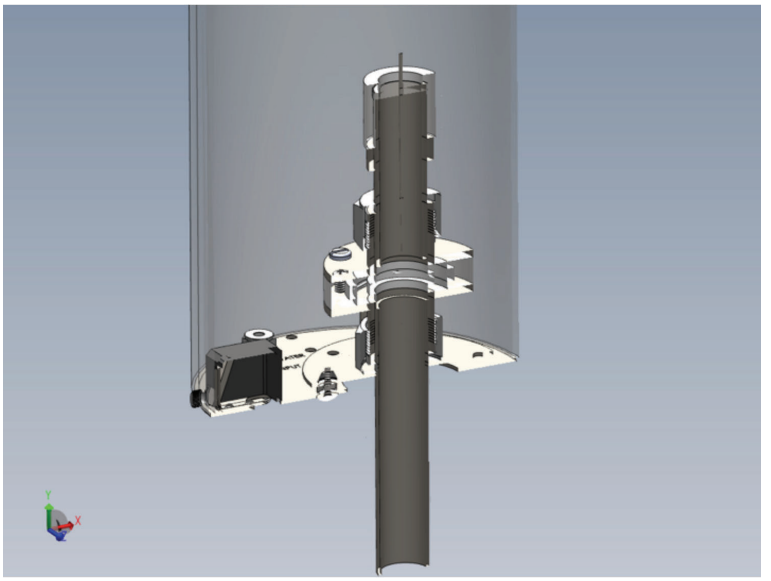

FIG. 2: Three-dimensional drawing of the slice-through of the forward-vortex plasmatron system

3014C oscilloscope to obtain instantaneous readings during the operation of the plasmatron. Compressed air and carbon dioxide were fed tangentially into the plasmatron at 0.4, 0.6, 0.8, and 1.0 SCFM while plasma was ignited. Calculation of total energy consumption and duration of single pulse reading was performed with MATLAB. Total energy can be calculated using the equation below, where V, I, and P are the instantaneous voltage, current, and power, respectively. The product of the actual voltage and current yields instantaneous power and the integral of power over the total time yields total energy.

$$V(t)^* I(t) = P(t)$$

$$\int_0^T P(t)dt = E$$

Single pulse readings were then conducted by changing the time step on the oscilloscope to 2.00 ms and then recording the data points. The approximate times when the pulse initialized and finalized were then determined through approximation and those sets of points were cropped out from the whole data set. This new data set was then analyzed in MATLAB by calculating instantaneous power and total energy.

C. Thermal Characterization

An OMEGA L-0044T thermocouple connected to a FLUKE 5211 thermocouple thermometer was used to take temperature readings of the plasmatron system above the ring electrode. Carbon dioxide gas from a cylinder and pipelined compressed air were flowed through the plasmatron at flow rates of 0.4, 0.6, 0.8, and 1.05 SCFM and 0.3, 0.4, 0.5, and 0.6 SCFM, respectively. Temperature measurements were taken at time intervals of 10 s for the first minute followed by intervals of 30 s until a total run time of 5 min was reached.

D. Water Analysis

For water analysis, a Fusion One Syringe Infusion Pump by Chemyx Inc. was used to regulate flow rate of water injected from a Monoject 60 ml, 2 oz syringe. To determine pH and nitrate levels in plasma-treated water, a Thermo Scientific Orion Dualstar pH/ISE Benchtop was used along with Thermo Scientific Orion 9700BNWP Handle for Ion+Combination ISE Electrode, Thermo Scientific Orion 900200 Sure-Flow Reference Half-Cell Electrode, and a Thermo Scientific Orion 8220BNWP PerpHecT Ross Combination Micro pH Electrode. Water loss was documented by varying both the air flow rate and water flow rate into the plasmatron. Water loss vs. water flow rate was performed by maintaining the air flow rate at 1 SCFM while varying the water flow rate at 16.7, 20.0, 25.0, 33.3, and 50.0 ml/min. Water loss vs. air flow rate was conducted by keeping the

water flow rate constant at 50 ml/min and varying the air flow rate at 0.6, 0.8, 1.0, and 1.2 SCFM.

Plasma-generated acidified water was produced at 16.7 ml/min @ 1 SCFM, 50 ml/min @ 1 SCFM, and 0.8 SCFM @ 50ml/min. To determine total water loss from heat generated by the system, the treated water was placed onto a 140-mm aluminum weighing dish and weighed with a Fisher Scientific Accu-64 scale. The pH and nitrate levels were also immediately measured after each weigh. Samples of water are stored in separate sets of BD Falcon Centrifuge tubes. Two separate sets of samples were produced by storing some with an air bubble in the tube and another without. The pH and nitrate level readings of both sets were taken immediately and also after letting the samples rest for 1 h and 48 h.

E. Photo and Video Recording

To document plasma behavior with photographs and video we have used a digital single-lens reflex camera (Nikon D800E, Nikon, USA) with macro lens (Nikon AF-S VR Micro-Nikkor 105 mm *f*/2.8G IF-ED, Nikon, USA) and a macro conversion lens (Raynox DCR-5320PRO with Bower 62–72-mm step-up ring, distributed by B&H Photo, Video, & Pro Audio, New York, NY). Figure 3 shows a photograph of the setup used to document the plasmatron. The photography setup remained approximately the same throughout all the experiments reported on in this document.

FIG. 3: Photograph of the setup used to photographically document plasmatron (white bar represents 25.4 mm)

III. RESULTS

A. Electrical and Thermal Characterization

From the data received from MATLAB calculations of 1 pulse of compressed air over 0.4, 0.6, 0.8, and 1.0 SCFM, energy increases as air flow rate increases. This increase is also apparent in 1 pulse CO_2 results. However, it is also noted that energy consumption for the plasmatron with CO_2 flow is much greater than with compressed air flow. There also does not seem to be any correlation between the gas flow rate and the length of each pulse. These findings are demonstrated in the results shown in Tables 1 and 2.

As the compressed air flow rate is increased, energy consumption of the plasmatron over 1 s and 1 pulse also increases accordingly as shown in Figure 4. As CO_2 flow rate is increased, energy consumption is increased over 1 s readings but interestingly no energy-gas flow rate correlation can be determined over 1 pulse duration as shown in Figure 5, for oscillograms used in this analysis, see Figures 6-9.

As expected, when measuring the temperature of the plasmatron with an OMEGA L-0044T Thermocouple connected to a FLUKE 5211 Thermocouple thermometer, an increasing trend is determined from the measurements. Interestingly, the lowest gas flow rate for CO_2 and compressed air (0.3 and 0.4 SCFM, respectively) yields the highest final temperature, while the higher gas flow rates yield a lower temperature after 300 s of continuous run time of the system. See Figures 10 and 11.

B. Thermal Characterization

We analyze the rise of the temperature of the high voltage electrode during the system operation. Unfortunately, given the current configuration of the plasma system we see temperature rise as much as 60°C in 5 min of operation. Clearly, this issue needs to be addressed in an industrial setting either by actively cooling the electrodes (air-cooling or water-cooling are both possible and have been introduced before) or by other modifications leading to reduced time of contact of the arc with the electrode and better gas flow arrangement to allow for longer operating times.

C. Water Characterization

With an initial water volume of 50 ml, it was determined that volume of water loss increases as compressed air flow rate increases. Interestingly, volume of water loss decreases as water flow rate increases as shown in Figure 12.

Chemistry of the treated water also changes with low water flow and high water

TABLE 1: Chart of comparison between CO_2 flow rates with energy consumption per pulse and length per pulse

Flow rate (SCFM)	Energy (J)	Length of pulse (ms)
0.4	0.9686	1.090
0.6	1.4961	1.520
0.8	0.9283	1.822
1.0	0.8427	0.843

TABLE 2: Chart of comparison between compressed air flow rates with energy consumption per pulse and length per pulse

Flow rate (SCFM)	Energy (J)	Length of pulse (ms)
0.4	0.2683	3.000
0.6	0.4581	3.578
0.8	0.5525	4.630
1.0	0.6833	4.458

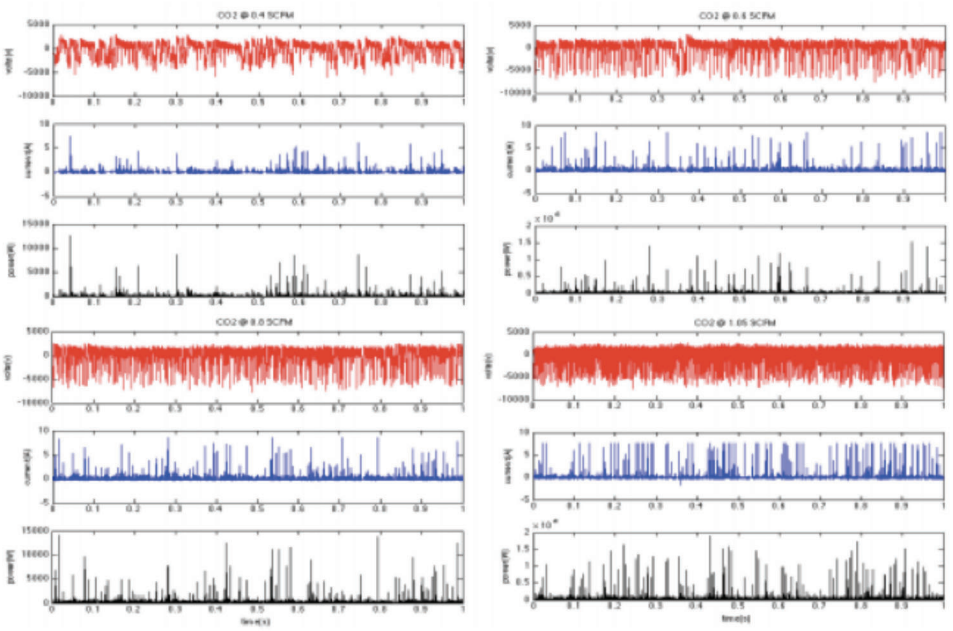

FIG. 4: *I-V-P* readings for CO_2 with instantaneous power over 1 s

flow. Initial pH of untreated tap water is at 7.944. The pH of water that was treated under 16.7 ml/min yielded a pH of 7.1365 while pH of water treated under 50 ml/min yielded a pH of 6.8915 as shown in Figure 13. Interestingly, pH of the low flow rate sample increased as the high flow rate sample decreased at 24 h and then increased at 48 h. The no-air-gap samples of both flow rates yielded no significantly distinct

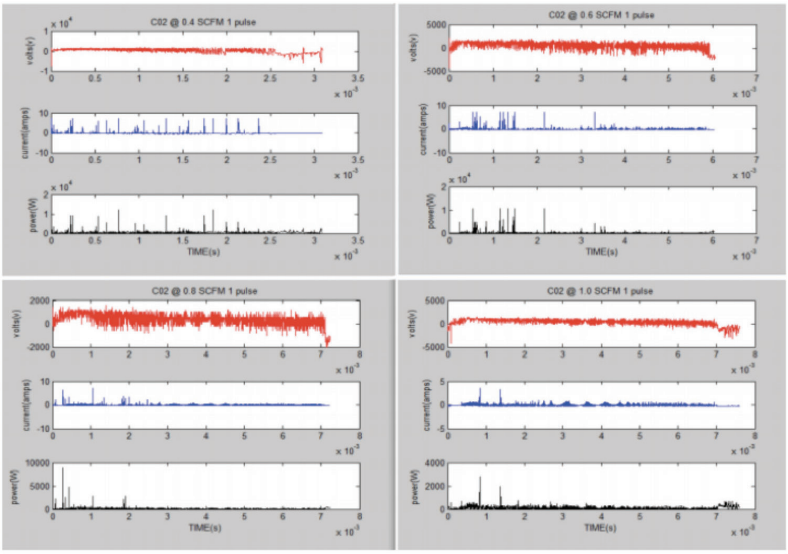

FIG. 5: *I-V-P* readings for CO_2 with instantaneous power over 1 pulse

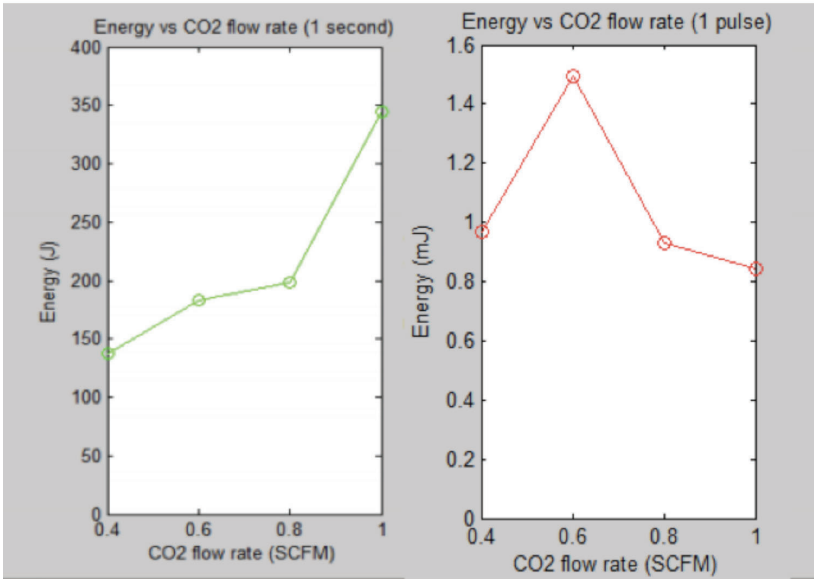

FIG. 6: Energy readings for CO_2 with 0.4–1.0 SCFM flow rate over 1 s and 1 pulse, respectively

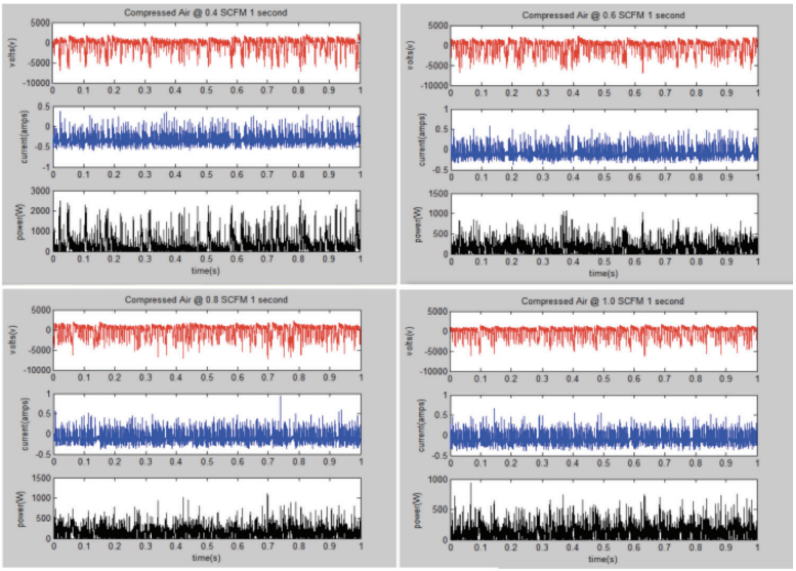

FIG. 7: *I-V-P* readings for compressed air with instantaneous power over 1 s

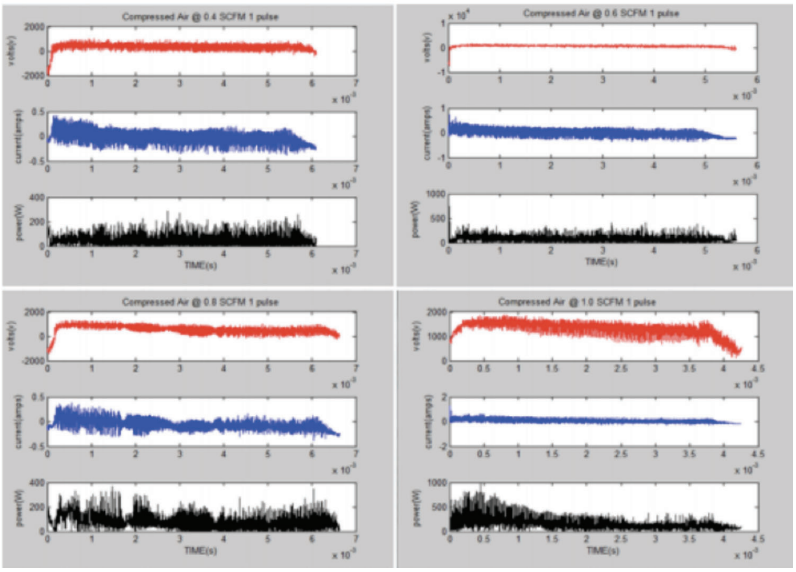

FIG. 8. *I-V-P* readings for compressed air with instantaneous power over 1 pulse

results from the air-gap samples.

Initial nitrate concentration of untreated tap water is at 1.75 mg/l. When water is treated at 16.7 ml/min, nitrate level yields 4.00 mg/l while water treated at 50 ml/min yields a nitrate concentration of 3.215 mg/l. Interestingly, nitrate levels for both

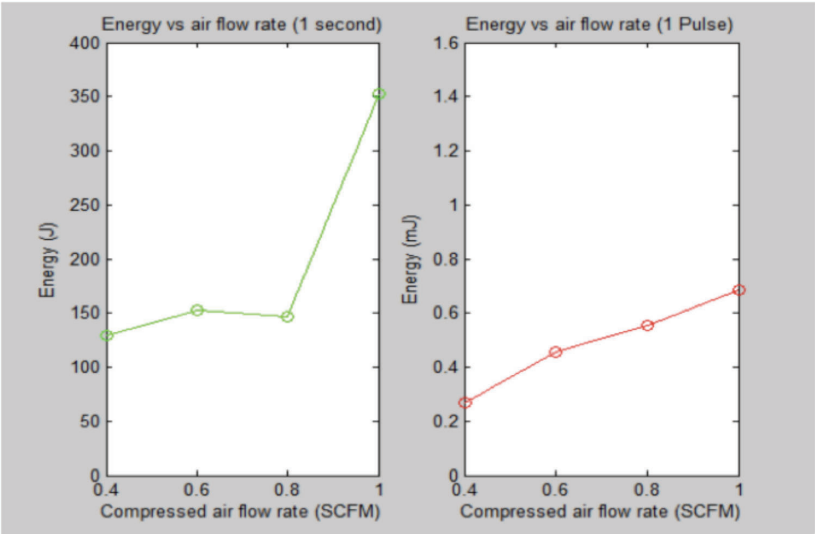

FIG. 9: Energy readings for compressed air with 0.4–1.0 SCFM flow rate over 1 s and 1 pulse, respectively

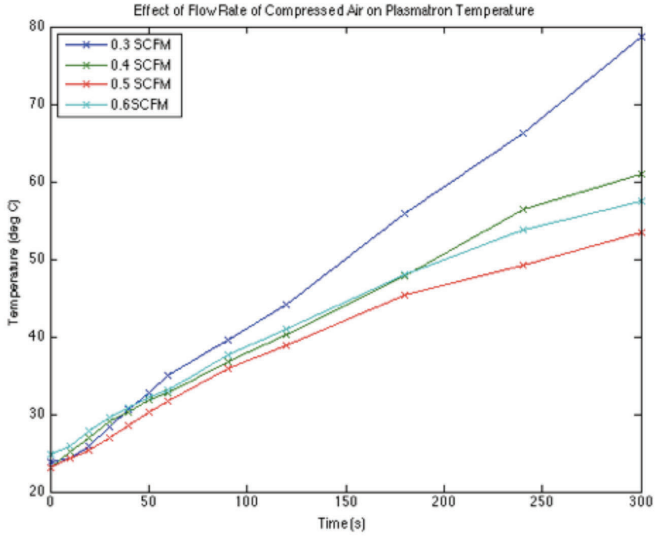

FIG. 10: Plot of temperature readings obtained at various flow rates of compressed air

high and low flow rates increase over 24 h but decrease at 48 h. Low flow with air exposed, low flow without air exposed, and high flow with air exposed yielded similar results at 24 h (5.86–5.76 mg/l) but after 48 h, high water flow with air exposed yielded

the highest concentration of nitrates out of all the samples during that time at 5.025 mg/l. These measurements of the stability of nitrate concentration as well as stability of other compounds of interest can be found in Figures 14-17.

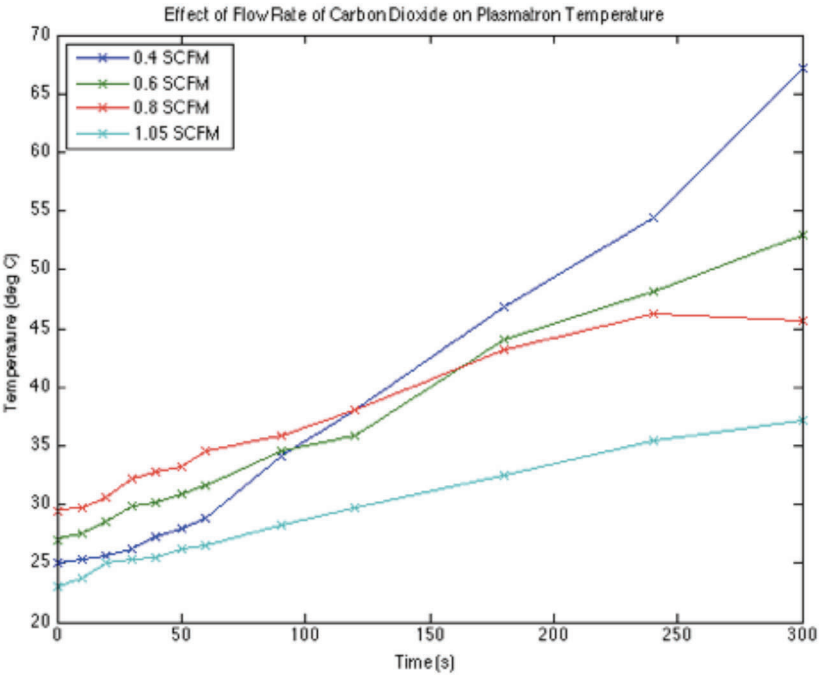

FIG. 11: Plot of temperature readings obtained at various flow rates of CO_2

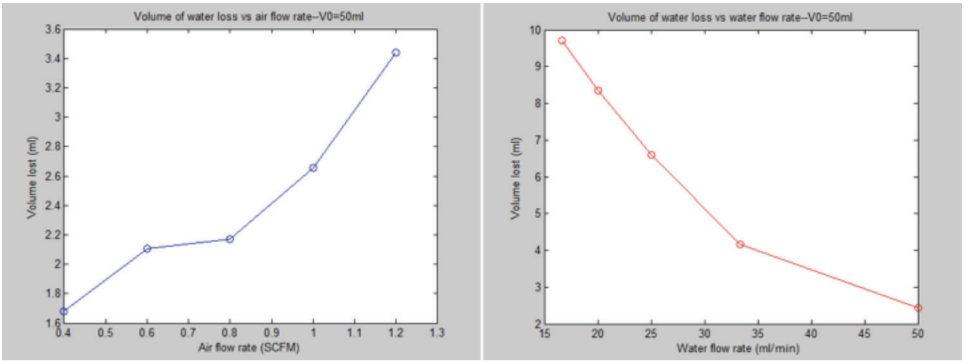

FIG. 12: Plot of water loss vs. air flow rate (SCFM) and water flow rate (ml/min)

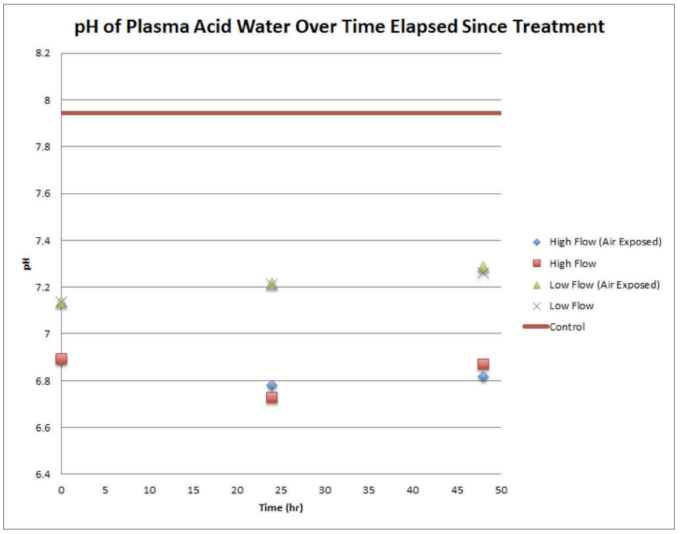

FIG. 13: Plot of pH levels vs. time in plasma-treated tap water over t=0, t=1, and t=48 h. Samples with water flow rates of 16.7 and 50 ml/min were analyzed. Samples with air exposed and no air exposed were also analyzed.

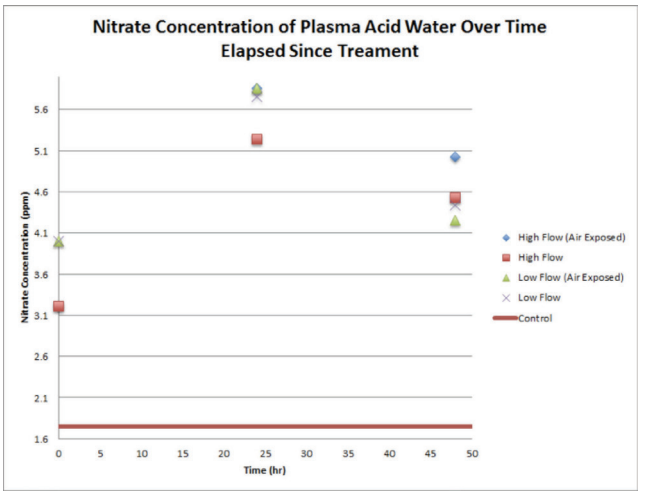

FIG. 14: Plot of nitrate concentration vs. time in plasma-treated tap water over t=0, t=1, and t=48 h. Samples with water flow rates of 16.7 and 50 ml/min were analyzed. Samples with air exposed and no air exposed were also analyzed.

As can be expected from a thermal plasma generated in atmospheric air in the presence of water, Figure 18 shows an abundance of nitrogen lines in the discharge emission.

D. Photographs of the Discharge Development

Figure 19 shows a sequence of photographs of the discharge development from the initial thermal arc to the elongated and twisted transitional arc, filling most of the central volume, to finally extinguishing and reigniting. In burst mode, this camera is capable of approximately 12 images per second; thus the time interval between these shots is approximately 80 ms and it is clearly visible that the individual gliding arc exists for approximately half of a second. It can also be observed that thne new arc ignites when

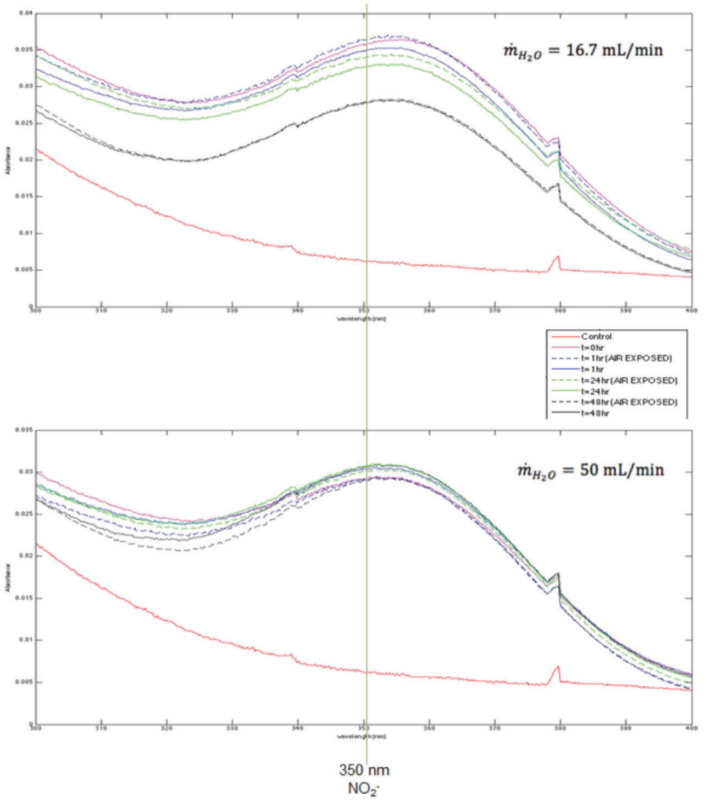

FIG. 15: UV VIS analysis of plasma-treated water injected at 16.7 and 50 ml/min into the plasmatron. Shows nitrite levels at 350 nm

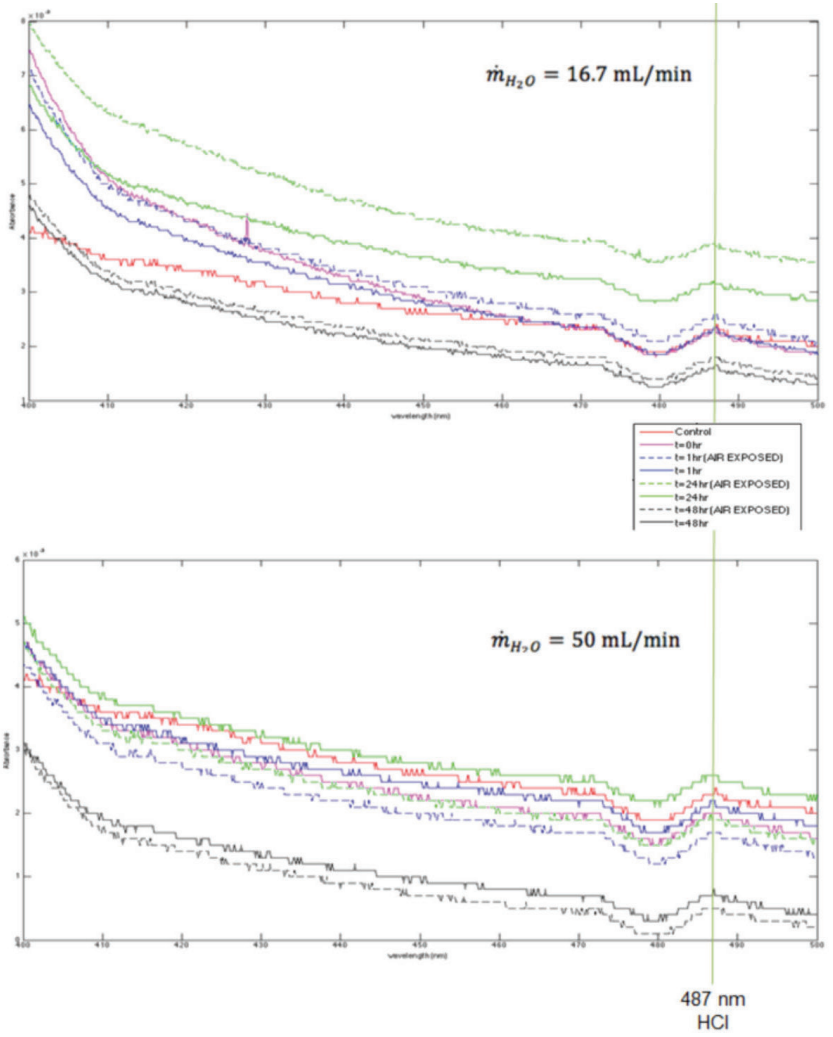

FIG. 16: UV VIS analysis of plasma treated water injected at 16.7 ml/.min and 50 ml/min into the plasmatron. Shows HCL levels at 487nm.

the previous arc is disconnected from the electrodes.

IV. DISCUSSION AND CONCLUSION

In this paper we have discussed treatment of water by the nonequilibrium atmospheric pressure forward-vortex plasma system and the generation of various reactive species in the flowing water. The key advantage of such system is that the water is moving through

plasma without contact with the electrodes and allows for generation of a reasonably high volume of the treated water. We have discussed the design of a new forward-vortex system and showed how the discharge interacts with the gas flow and the liquid flow. We presented current, voltage, and power characteristics of this system. The presented plasma system does overheat (up to 80°C) in just 5 min of operation which clearly would present a problem in an industrial setting. We have suggested possible solutions to this problem that we also plan to investigate in the near future. We have discussed the drop in pH and increase in nitrate concentration of the plasma-treated water and its dependence

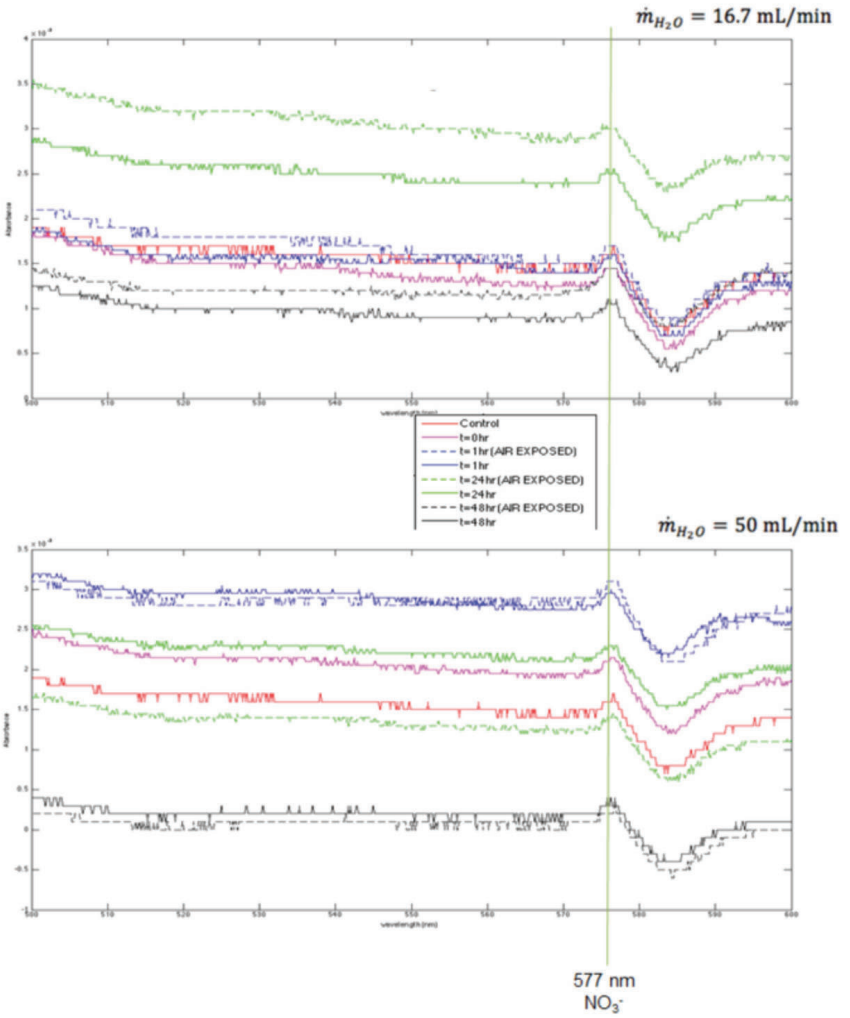

FIG. 17: UV VIS analysis of plasma-treated water injected at 16.7 and 50 ml/min into the plasmatron. Shows nitrate levels at 577 nm

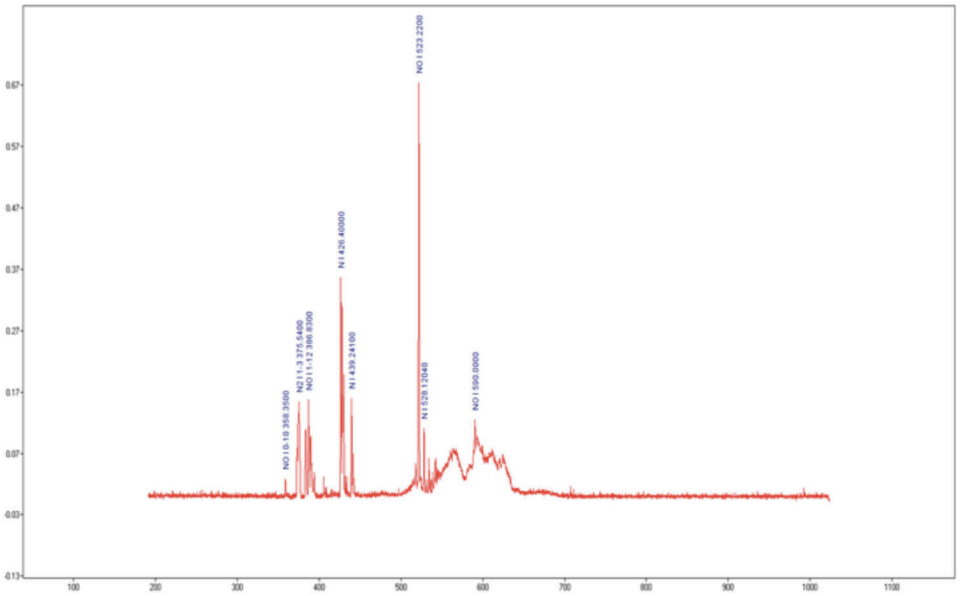

FIG. 18: Optical emission spectra of the gliding arc plasmatron operating with compressed air

on both the water and the carried gas flow rate.

Clearly, many unanswered questions remain to be studied to industrialize the treatment of flowing water by forward or forward-vortex plasmatrons. This paper presents initial steps in development of these systems and we hope to further focus on the issues of electrode overheating, increasing the flow rates while maintaining lowered pH, and other industrially important challenges.

REFERENCES

1. Zhuwen Z. Introduction of a new atmospheric pressure plasma device and application on tomato seeds. Agric Sci. 2011:2(1):23–7.
2. Zhang R, Wang L, Wu Y, Guan Z, Jia Z. Bacterial decontamination of water by bipolar pulsed discharge in a gas-liquid-solid three-phase discharge reactor. IEEE Trans Plasma Sci. 2006:34(4):13704.
3. Young Sun M, Jin OJ, Whitehead JC. Degradation of an azo dye Orange II using a gas phase dielectric barrier discharge reactor submerged in water. Chem Eng J. 2008:142:56–64.
4. Yang Y, Kim H, Starikovskiy A, Fridman A, Cho YI. Pulsed multichannel discharge array in water with stacked circular disk electrodes. IEEE Trans Plasma Sci. 2011:39(11):2624–5.
5. Yang Y, Gutsol A, Fridman A, Cho Y. Removal of CaCO3 scales on a filter membrane using plasma discharge in water. Int J Heat Mass Transfer. 2009:52(21-22):4901–6.
6. Starikovskiy A, Yang Y, Cho YI, Fridman A. Non-equilibrium plasma in liquid water: dynamics of generation and quenching. Plasma Sources Sci Technol. 2011:20(2):024003.

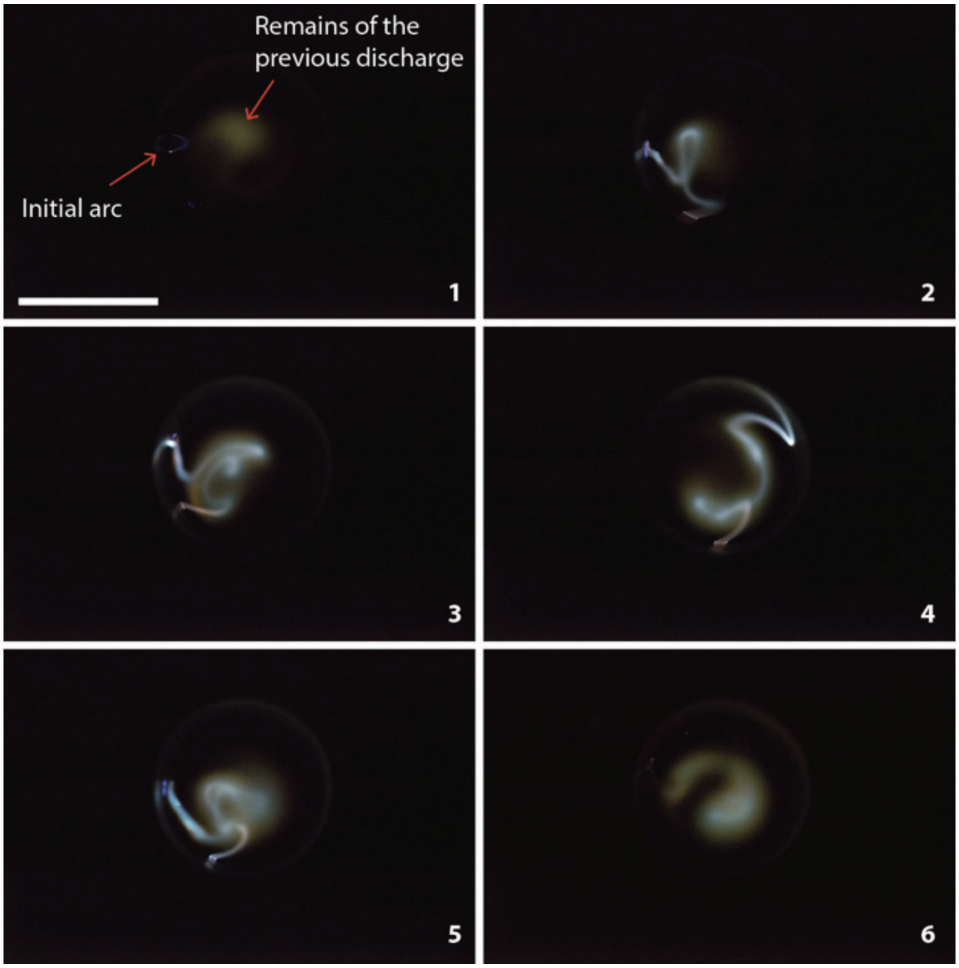

FIG. 19: Sequence of photographs of the discharge development (white bar represents 25.4 mm).

7. Sera B, Gajdova I, Cernak M, Gavril B, Hnatiuc E, Kovacik D, Kriha V, Sláma J, Sery M, Spatenka P. How various plasma sources may affect seed germination and growth. In: 13th International Conference on Optimization of Electrical and Electronic Equipment (OPTIM), 2012. New York: IEEE; 2012. p. 1365–70.
8. Oehmigen K, Hähnel M, Brandenburg R, Wilke Ch, Weltmann K-D, von Woedtke Th. The role of acidification for antimicrobial activity of atmospheric pressure plasma in liquids. Plasma Process Polym. 2010;7:250–7.
9. Scholtz V, Julak J, Kriha V. The microbicidal effect of low-temperature plasma generated by corona discharge: comparison of various microorganisms on an agar surface or in aqueous suspension. Plasma Process Polym, 2010;7(3-4):237–43.
10. Machala Z, Chladekova L, Pelach M. Plasma agents in bio-decontamination by dc discharges in atmospheric air. J Phys D Appl Phys. 2010;43(22): 222001.
11. Yudelevich I, Zaksas B, Petrova YA, Cherevko A. Analysis of atmospheric particular matter and water

using atomic emission spectrometry with inductively-coupled plasma and two-jet plasmatron. Fresen J Anal Chem. 1991;340(9):560–3.
12. Burlica R, Kirkpatrick MJ, Locke BR. Formation of reactive species in gliding arc discharges with liquid water. J Electrostat. 2006;64:35–43.
13. Laroussi M, Nonthermal decontamination of biological media by atmospheric-pressure plasmas: Review, analysis, and prospects. IEEE Trans Plasma Sci. 2002:30(4):1409–15.
14. Moisan M, Barbeau J, Crevier M-C, PelletierJ, Philip N, Saoudi B. Plasma sterilization. Methods and mechanisms. Pure Appl Chem. 2002;74(3):349–58.
15. Locke B, Sato M, Sunka P, Hoffmann M, Chang J-S. Electrohydraulic discharge and nonthermal plasma for water treatment. Indust Eng Chem Res. 2006;45(3):882–905.
16. Hayashi N, Guan W, Tsutsui S, Tomari T, Hanada Y. Sterilization of medical equipment using radicals produced by oxygen/water vapor RF plasma. Jpn J Appl Phys. 2006:45(10S):8358–63.
17. Kelly-Wintenberg K, Hodge A, Montie T, Deleanu L, Sherman D, Roth JR, Tsai P, Wadsworth L. Use of a one atmosphere uniform glow discharge plasma to kill a broad spectrum of microorganisms. J Vac Sci Technol A. 1999:17(4):1539–44.
18. Laroussi M. Sterilization of contaminated matter with an atmospheric pressure plasma. IEEE Trans Plasma Sci. 1996:24(3):1188–91.
19. Hong YC, Park HJ, Lee BJ, Kang W-S, Uhm HS. Plasma formation using a capillary discharge in water and its application to the sterilization of E. coli. Phys Plasmas. 2010;17(5):053502–053502-5.
20. Uhm HS, Lim JP, Li SZ, Sterilization of bacterial endospores by an atmospheric-pressure argon plasma jet. Appl Phys Lett. 2007:90(26):261501.
21. Lee K., Paek K-h, Ju W, Lee Y. Sterilization of bacteria, yeast, and bacterial endospores by atmospheric-pressure cold plasma using helium and oxygen. J Microbiol Seoul. 2006:44(3):269.
22. Cvelbar U, Vujoševič D, Vratnica Z, Mozetič M. The influence of substrate material on bacteria sterilization in an oxygen plasma glow discharge. J Phys D Appl Phys. 2006:39(16):3487–93.